Biochemical Pharmacology, Vol. 51, pp. 1569–1577, 1996.

ISSN 0006-2952/96/$15.00 + 0.00
PII S0006-2952(96)00101-3

Iron Coordination by Catechol Derivative Antioxidants

Teruyuki Kawabata, Victor Schepkin, Nobuya Haramaki, Ratna S. Phadke† and Lester Packer*

MEMBRANE BIOENERGETICS GROUP, DEPARTMENT OF MOLECULAR AND CELL BIOLOGY, UNIVERSITY OF CALIFORNIA, BERKELEY, CA 94720-3200, U.S.A.

ABSTRACT. Iron complexes of nitrocatechols with different substituent groups [**1**: $-CH=CR_2$; **2**: $-CH_2-CHR_2$; **3**: $-CH=CR'(R'')$] were synthesized and their effects on iron-induced free radical reactions of biological importance investigated. Catechol and nitrocatechol derivatives effectively inhibited iron-induced lipid peroxide-dependent lipid peroxidation. In the Fenton-like reaction, iron-catechol generated hydroxyl radicals more strongly than did iron citrate, and iron-nitrocatechol derivative **2** generated a small amount of hydroxyl radicals. The iron complexes of derivatives **1** and **3** did not generate hydroxyl radicals. Iron-catechol had the highest ratio of reduction to oxidation rate constants and the second was iron-nitrocatechol **2**, suggesting that iron chelated by nitrocatechols **1** and **3** may be most difficult to reduce. To elucidate the structure and physical properties of the iron complexes, UV/vis absorption spectroscopic, ESR and ^1H NMR studies were performed in aqueous and DMSO solutions. In aqueous solution at pH 7.4, iron complexes of the nitrocatechol derivatives were high-spin tris(nitrocatecholato)ferrate(III) with a characteristic ligand-to-metal charge transfer absorbance ($\pi \rightarrow d_\pi$). The λ_{max} of iron-nitrocatechol derivative **2** was shorter than those of iron-nitrocatechol derivatives **1** and **3**, suggesting that the reduction potential of iron-nitrocatechol **2** is higher than that of iron-nitrocatechols **1** and **3**. Nitrocatechol derivatives with a conjugation structure can sequester the chelated iron more effectively than catechol and the derivative without the conjugation against free radical generation by keeping the iron in the ferric state, probably because of the reduction potentials. BIOCHEM PHARMACOL 51;11:1569–1577, 1996.

KEY WORDS. chelation; lipid peroxidation; free radicals; reduction potential

It is well established that free radicals and active oxygen species are associated with many pathological conditions such as radiotherapy, ischemia–reperfusion, inflammation, and aging, where iron plays an important role by way of the generation of active oxygen species and free radicals [1–4]. Hydroxyl and alkoxyl radicals are believed to be major causative species for iron-induced free radical injuries in biological systems [5]:

$$H(L)OOH + Fe^{2+} \rightarrow H(L)O^{\cdot} + OH^- + Fe^{3+}$$

Although other reactive intermediates such as oxoferryl complex and binuclear peroxo complex are also proposed in the process of iron-catalyzed activation of oxygen [6–8], ferrous ion may be potentially much more dangerous than ferric ion. Since iron exists as a chelated complex in biological conditions [9, 10], if iron can be kept ferric by a chelator under physiological conditions, the catalytic activity of iron for free radical reactions will be decreased, suggesting the significance of a low reduction potential of an iron chelator complex. Transferrin and desferal (methanesulfonate salt of desferrioxamine B, a siderophore of the hydroxamate type) are widely used for protection against iron-induced free radical injuries. They are strong chelators for iron ($pK_f \approx 30$),‡ and their iron complexes have much lower reduction potential ($E° \approx -0.3$ V) than other iron chelators such as EDTA, citrate, and ADP [11].

From a clinical viewpoint, the kind of chelator necessary to sequester catalytic iron in biological systems is an important question for disease protection and therapy. First of

* Corresponding author (and present address): Dr. Teruyuki Kawabata, Department of Pathology, Okayama University Medical School, 2-5-1 Shikata-cho, Okayama 700, Japan. Tel. +81-86-235-7145, Ext. 2330; FAX +81-86-221-4743.

† Permanent address: Chemical Physics, Tata Institute of Fundamental Research, Homi Bhabha Road, Bombay 400005, India.

Received 17 July 1995; accepted 26 December 1995.

‡ *Abbreviations:* K_f, formation constant; k, rate constant; s, d, t, and br, singlet, doublet, triplet, and broad; nitrocat, nitrocatechol derivative; TBARS, thiobarbituric acid reactive substance; DHLA, dihydrolipoic acid; DMPO, 5,5-dimethyl-1-pyrroline-*N*-oxide; DMPO-OH, hydroxyl radical adduct of DMPO; DPPH, 2,2-di(4-*tert*-octylphenyl)-1-picrylhydrazyl; TMS, tetramethylsilane; TSP, sodium 3-trimethyl[2,2,3,3-D_4]propionate; and HOMO, highest occupied molecular orbital.

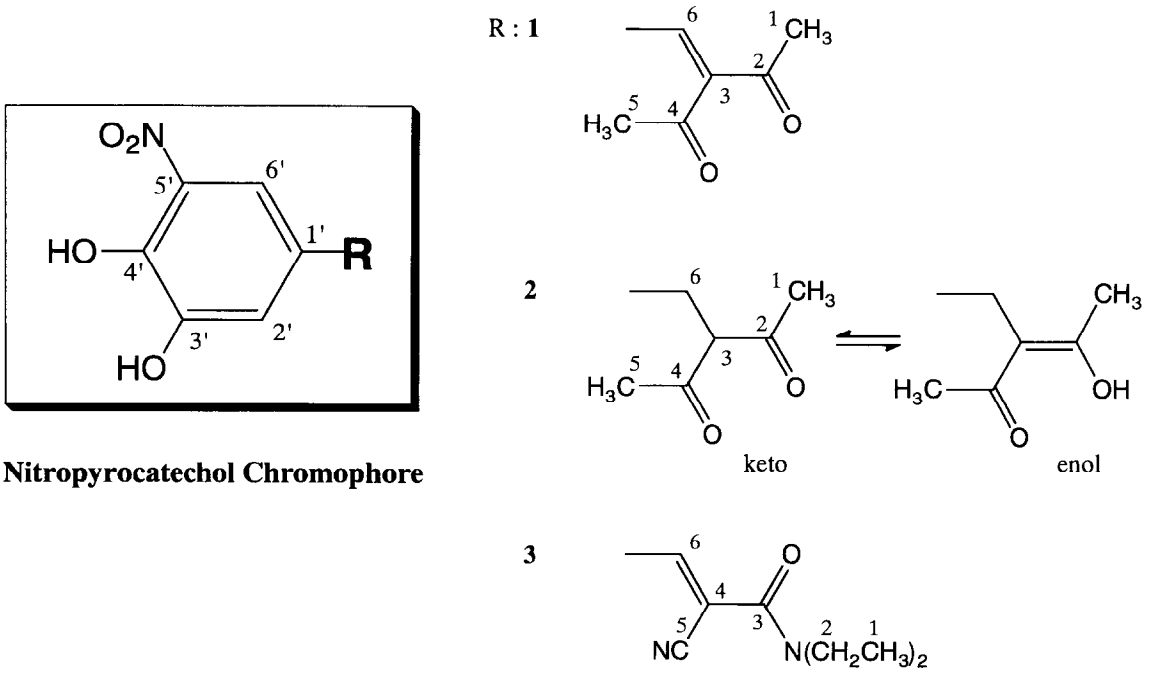

FIG. 1. Catechol derivative antioxidants. The catechol derivatives have nitropyrocatechol chromophores in common, and the tail portions were different between the derivatives. Key: (1) 3-(3,4-dihydroxy-5-nitrobenzylidene)-2,4-pentanedione, (2) 3-(3,4-dihydroxy-5-nitrobenzyl)-2,4-pentanedione, and (3) 2-cyano-3-(3,4-dihydroxy-5-nitrophenyl)-N,N-diethyl-2-propenamide.

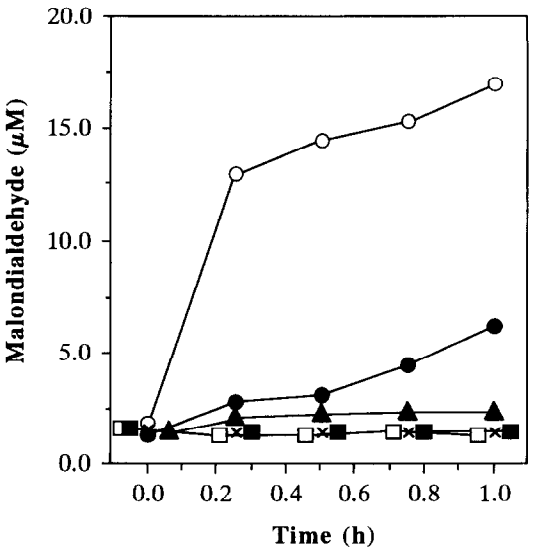

FIG. 2. Iron-induced lipid peroxide-dependent lipid peroxidation. Microsomes (1.0 mg protein/mL) were incubated with iron complexes of the nitrocatechol derivatives (0.1 mM iron and 0.3 mM chelators) and ascorbate (0.5 mM) in HEPES-saline (pH 7.4) at 37°, and lipid peroxidation was measured by the thiobarbituric acid method. Values are presented as malondialdehyde by using malonaldehyde bis(dimethyl acetal) as a standard. Key: (●–●) control; (○–○) citrate; (■–■) derivative 1; (□–□) derivative 2; (×–×) derivative 3; and (▲–▲) catechol. Values present averages in duplicate.

all, the chelator must form a stable iron complex to remove deleterious iron from biomolecules. However, in addition to thermodynamic stability, the reduction potential of the iron chelator is important for protection against iron-induced free radical injuries. Catechol-type chelators have large stability constants for iron and low reduction potentials [12, 13]. Catechol forms a thermodynamically stable complex with iron (log K_f = 40) as a bidentate ligand [14] and has been crystallized as an octahedral complex [tris(catecholato)ferrate(III)] [15]. Catechol-type chelators are used as siderophores by microorganisms like hydroxamate-type chelators, such as desferrioxamine B [16], and may not be so toxic to cells. Recently, a nitrocatechol derivative [3-(3,4-dihydroxy-5-nitrobenzylidene)-2,4-pentanedione] was reported to be a potent antioxidant [17, 18]. The nitrocatechol derivative antioxidant was applied to ischemia–reperfusion injuries of rat heart [19], in which we showed effective protection against the injuries and suggested some chelating effects of the derivative for protection in addition to the radical scavenging effects.

In the present study, iron-induced lipid peroxidation and hydroxyl radical generation were tested in the presence of nitrocatechol derivatives, and the oxidation and reduction rates of the iron chelated by the derivatives were also studied in aqueous solution. To elucidate the molecular environment around the iron, the physical properties of iron–nitrocatechol derivative complexes were studied by UV/vis absorption, ESR and NMR spectroscopy. It was clarified that nitrocatechol derivatives formed catechol-type complexes with iron and were effective for the protection against iron-induced free radical reaction.

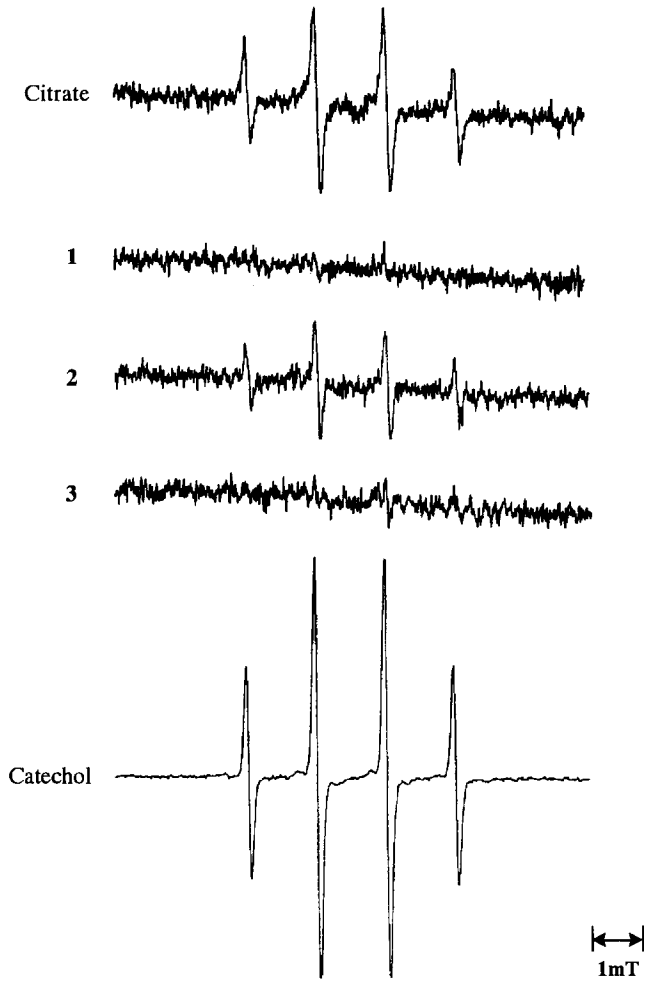

FIG. 3. ESR spin-trapping of hydroxyl radicals generated by iron complexes of nitrocatechol derivatives 1, 2, and 3 (shown in Fig. 1) and H_2O_2. The reaction was done at room temperature in the presence of iron complexes (0.33 mM iron and 1 mM chelator), hydrogen peroxide (500 mM), and DMPO (100 mM). ESR spectra were taken 10 min after the addition of hydrogen peroxide. Gain: 5.0 × 10^5 except for catechol (gain: 1.0 × 10^5).

MATERIALS AND METHODS

Reagents

Nitrocatechol derivatives were gifts from Orion–Farmos Pharmaceuticals (Espoo, Finland) (Fig. 1): **(1)** 3-(3,4-dihydroxy-5-nitrobenzylidene)-2,4-pentanedione, ^{1}H NMR (DMSO-d_6) δ 2.38 (s, 3H), 2.26 (s, 3H), 7.09 (d, 1H), 7.57 (s, 1H), 7.60 (d, 1H), 10.7 (br, 1H); **(2)** 3-(3,4-dihydroxy-5-nitrobenzyl)-2,4-pentanedione, keto(enol) type, ^{1}H NMR (DMSO-d_6) δ 2.07 (s, 1H), 2.14 (s, 1H), 2.92 (d, 1H) (3.58 (d, 1H)), 4.25 (t, 1H), 6.93 (d, 1H) (6.89 (d, 1H)), 7.21 (d, 1H) (7.10 (d, 1H)), 10.08 (br, 1H) (16.86 (br, 1H)); and **(3)** 2-cyano-3-(3,4-dihydroxy-5-nitrophenyl)-*N*,*N*-diethyl-2-propenamide, ^{1}H NMR (DMSO-d_6) δ 1.16 (s, 6H), 3.41 (s, 4H), 7.65 (s, 1H), 7.76 (d, 1H), 7.93 (d, 1H), 10.92 (br, 1H). Catechol, citrate (trisodium salt), deferoxamine methylate (Desferal), HEPES, bovine serum albumin (fraction V, essentially fatty acid free) and DMSO were purchased from the Sigma Chemical Co. (St. Louis, MO). Malonaldehyde bis(dimethyl acetal), DMPO and gallium(III) nitrate hydrate were purchased from the Aldrich Chemical Co. (Milwaukee, WI). DMPO was used after purification with charcoal [20]. D_2O and DMSO-d_6 were from Wilmad (Buena, NJ) and $Fe(NO_3)_3 \cdot 5H_2O$ was from J. T. Baker Chemical (Phillipsburg, NJ). L-Ascorbic acid was obtained from Fisher Scientific (Pittsburgh, PA). All other reagents were analytical grade.

Male Sprague–Dawley rats (200–250 g) were obtained from Bantin & Kingman (Fremont, CA) and acclimatized for at least 3 days with *ad lib.* access to standard laboratory food and water.

Lipid Peroxidation of Rat Liver Microsomes

Rat liver was homogenized in a medium (220 mM mannitol, 70 mM sucrose, 2 mM HEPES, and 0.5 g/L bovine serum albumin) on ice, and then microsomes were prepared by centrifugation [21]. The protein concentration was measured as described by Lowry *et al.* [22], and microsomes (10.0 mg protein/mL) were resuspended in HEPES-saline (20 mM HEPES and 150 mM NaCl, pH 7.4). Ten microliters of $Fe(NO_3)_3$ (10 mM in 0.1 N HCl) and 300 μL of nitrocatechol derivative or citrate (1 mM in HEPES-saline) were added to 490 μL of HEPES-saline, and then 100 μL of

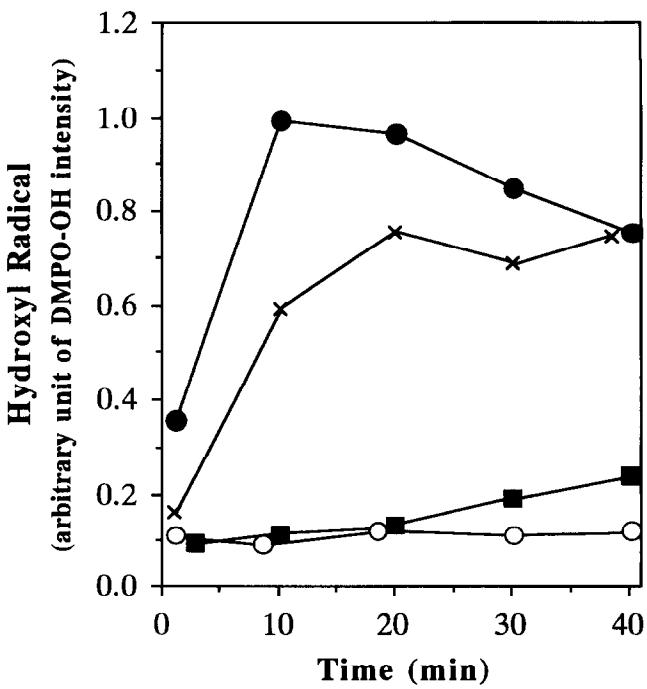

FIG. 4. Hydroxyl radical generation by iron complexes of nitrocatechol derivatives and H_2O_2. The intensity of the second line of DMPO-OH produced under the same conditions described in the legend of Fig. 3 was followed at room temperature. Key: (●–●) citrate; (○–○) derivative 1; (×–×) derivative 2; and (■–■) derivative 3. Values present averages in duplicate.

TABLE 1. Oxidation and reduction rate constants of iron in nitrocatechol derivative complexes

	k_{Ox} ($\times 10^{-3}$ $M^{-1} \cdot sec^{-1}$)	k_{Rd} ($M^{-1} \cdot sec^{-1}$)	k_{Rd}/k_{Ox} ($\times 10^3$)
Citrate	0.56 ± 0.07	0.84 ± 0.03	1.5
1	3.15 ± 0.06	0.20 ± 0.00	0.063
2	2.89 ± 0.01	0.20 ± 0.01	0.070
3	2.91 ± 0.07	0.18 ± 0.02	0.062
Catechol	2.34 ± 0.04	1.70 ± 0.16	0.73

The rate constants of oxidation (k_{Ox}) and reduction (k_{Rd}) were measured in HEPES-saline (pH 7.4) at 25°, assuming a saturated oxygen concentration of 253 μM, and the rate constants were calculated as a second-order reaction. Each value is the mean ± SD of four experiments.

microsomes was added and mixed. The reaction was started by the addition of 100 μL of ascorbate (5 mM in distilled water), and the reaction mixture was incubated at 37°. The reaction was stopped by the addition of 1.0 mL of Desferal (1 mM in distilled water), and TBARS was measured by the method of Ohkawa *et al.* [23]. Malonaldehyde bis(dimethyl acetal) was used as a standard for TBARS.

ESR Spin-Trapping

DMPO (100 mM) was used as a spin trap to detect hydroxyl radicals [6]. The reaction was initiated by the addition of hydrogen peroxide (500 mM) to ferric complexes (1 mM derivative and 0.33 mM iron). ESR spectra were recorded by a Varian E 109E spectrometer using 50-μL capillary tubes at room temperature under the following conditions: microwave power, 20 mW; gain, 5.0×10^5; modulation, 0.125 mT; scanning field, 348 ± 5 mT; sweep time, 50 sec; time constant, 100 msec.

Oxidation and Reduction Rates of the Iron

A Clarke-type oxygen electrode was used at 25°, assuming a saturated oxygen concentration of 253 μM. For the oxidation rate, 10 μL of $FeSO_4$ (50 mM) in 0.001 N HCl was added to 1.5 mL of nitrocatechol derivative (1 mM) in HEPES-saline (pH 7.4), and oxygen consumption was measured. The oxidation rate was calculated from the stoichiometry:

$$Fe^{2+} + 1/4O_2 + H^+ \rightarrow Fe^{3+} + 1/2H_2O$$

The oxidation rate constant (k_{Ox}) was calculated by dividing the oxidation rate of ferrous ion by iron and oxygen concentrations.

For the reduction rate, 10 μL of $Fe(NO_3)_3$ (50 mM) in 0.001 N HCl was mixed with 1.5 mL of nitrocatechol derivative (1 mM) in HEPES-saline (pH 7.4), and then 10 μL of dihydrolipoic acid (1.5 M in ethanol) was added to the reaction mixture. The oxygen consumption was measured, and the reduction rate was calculated from the stoichiometry [24]:

$$Fe^{3+} + 1/2DHLA \rightarrow Fe^{2+} + 1/2LA + H^+$$
$$Fe^{2+} + 1/4O_2 + H^+ \rightarrow Fe^{3+} + 1/2H_2O$$

Since the latter rate was much more rapid than the former, the reduction rate of iron is approximately equal to the oxygen consumption. The rate constant (k_{Rd}) was calculated by dividing the rate by iron and DHLA concentrations.

UV/vis Absorption Spectrophotometry

UV/vis spectra of ferric complexes of nitrocatechol derivatives were recorded by a Perkin–Elmer spectrophotometer (Norwalk, CT) at room temperature. To determine the molar ratio of iron to nitrocatechol derivative, Job's plotting was used in HEPES-saline (pH 7.4) and DMSO. Spectra were recorded, changing the molar ratio of ferric ion and the nitrocatechol derivatives, but keeping the total amount of iron and derivatives constant (0.1 mM in HEPES-saline; 10 mM in DMSO).

ESR Spectroscopy

ESR spectra were recorded using a Bruker IBM ER200 D-SRC electron spin resonance spectrometer at 200°K. Ali-

TABLE 2. Properties of electronic absorption spectra of iron complexes of nitrocatechol derivatives in HEPES-saline (pH 7.4) and DMSO

	HEPES-saline (pH 7.4)		DMSO	
	λ (nm) (κ (cm^{-1}))	ε ($\times 10^3$ $M^{-1} \cdot cm^{-1}$)	λ (nm) (κ (cm^{-1}))	ε ($\times 10^3$ $M^{-1} \cdot cm^{-1}$)
1	525 (19050)	1.65	665 (15040)	2.42
2	540 (18520)	1.44	700 (14290)	1.80
3	520 (19230)	1.63	660 (15150)	2.46

The wave length (λ) and wave number (κ) of ligand-to-metal charge transfer of iron nitrocatechol complexes were measured at room temperature in the buffer and DMSO. The molar extinction coefficient (ε) is presented as iron concentration.

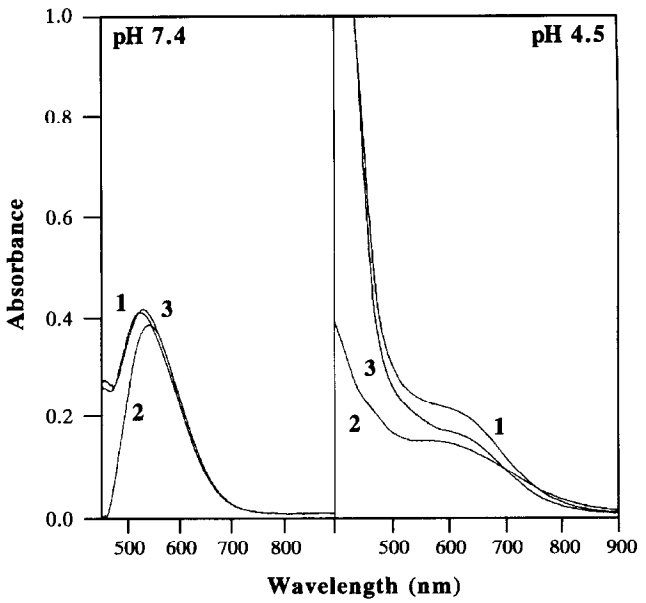

FIG. 5. Electronic absorption spectra of iron complexes of nitrocatechol derivatives in aqueous solution of different pH. Derivatives 1, 2, and 3 were 1.0 mM, and iron was 0.33 mM. Left: difference spectra in HEPES-saline (pH 7.4); right: spectra in 0.05 M acetate buffer (pH 4.5) of iron–nitrocatechols.

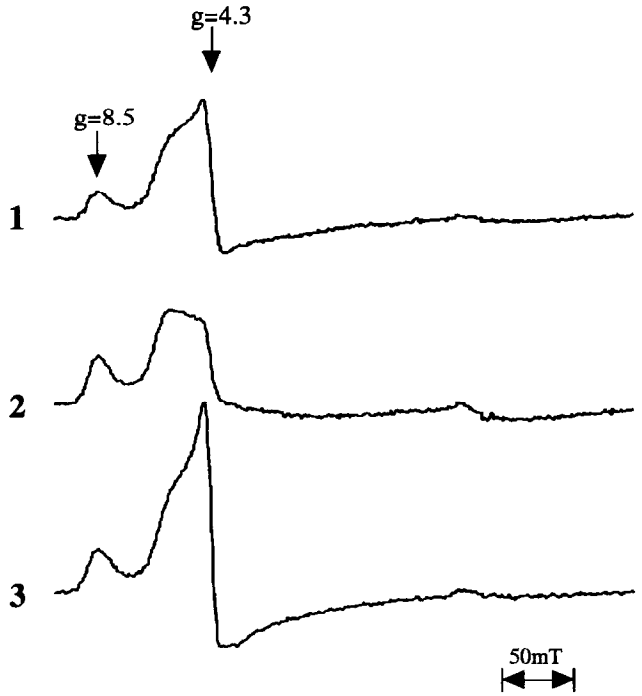

FIG. 6. ESR spectra of iron complexes of nitrocatechol derivatives. The ESR spectra of iron complexes of nitrocatechol derivatives 1, 2, and 3 (iron:derivative = 1:1) were recorded at 200°K in DMSO. The g values were measured by DPPH as a reference.

quots (500 μL) of iron complexes were frozen in liquid nitrogen and measured under the following conditions: power, 9.8 mW; modulation, 0.64 T; scanning field, 250 ± 200 mT; amplitude, 5.0×10^5; time constant, 500 msec; sweep time, 1000 sec. ESR spectra were analyzed by S = 5/2 spin Hamiltonian:

$$H = g_e \beta H_0 S + E (S_x - S_y) + D (S_z^2 - 35/12)$$

where g_e is 2.00, β is the Bohr magneton, H_0 is the external magnetic field, S (S_x, S_y, S_z) is the spin operator, and *E* and *D* are the zero-field splitting parameters [25].

NMR *Spectroscopy*

NMR data were obtained at room temperature in 5-mm sample tubes by a Bruker AM300-WB spectrometer. Chemical shifts were measured relative to TMS in DMSO and TSP in D_2O. Single pulse sequence was used for frequency region; sweep width, 8000 Hz (DMSO) and 3600 Hz (D_2O). The other parameters were: acquisition, memory size, 16 kbyte; number of scans, 64; duration of pulse, 8 μsec; relaxation delay, 3 sec. To study the structure of iron-nitrocatechols, Ga^{3+} was used as a substitute for Fe^{3+}. The pD was calculated by pD = pH + 0.4.

RESULTS

Iron-induced lipid peroxidation was studied using rat liver microsomes (Fig. 2). Microsomes incubated with iron and citrate produced lipid peroxidation, as measured by TBARS. Control microsomes also produced some TBARS, likely as a result of iron impurities in the microsomes. However, in the presence of nitrocatechol derivatives, iron did not promote lipid peroxidation in microsomes, and the lipid peroxidation was inhibited as compared with the control. Catechol also inhibited lipid peroxidation in the same manner as the derivatives. Using ESR spin-trapping, iron-catechol generated hydroxyl radicals much more strongly than did iron citrate, and iron-nitrocatechol derivative **2** generated a small amount of hydroxyl radicals (Figs. 3 and 4). However, iron complexes of derivatives **1** and **3** did not generate hydroxyl radicals.

The rates of oxidation and reduction were measured in

TABLE 3. Proton chemical shifts of Ga^{3+}-complexes of nitrocatechol derivatives in DMSO

^1H position on	Chemical shift (ppm) 1	2*	3
C1, C5(C2†)	2.37, 2.28	2.10	1.15, 3.40
C3		4.19	
C6	7.48	2.81	7.49
C2′, C6′	6.66, 7.44	6.53, 6.83	7.46, 7.67

The proton chemical shifts of Ga^{3+}-complexes of nitrocatechol derivatives in DMSO are presented relative to TMS. The proton positions are presented in Fig. 1 by numbering carbons to which the protons are bound.

* These chemical shifts are keto-type ones of iron-nitrocatechol complex.

† The chemical shift of the proton on C2 is presented in derivative **3** instead of the proton shift on C5.

TABLE 4. Proton chemical shifts of Ga^{3+}-complexes of nitrocatechol derivatives in D_2O (pD 7.5)

^1H position on	Chemical shift (ppm)					
	1	Δ	2	Δ	3	Δ
C1, C5	2.46, 2.43	−0.03, 0.00	2.22	−0.01	1.22	−0.02
C6	7.65	0.04	2.95	−0.03	7.48	0.01
C2′, C6′	6.72, 7.51	−0.12, −0.25	6.62, 7.02	−0.27, −0.22	7.44, 7.84	−0.17, −0.16

The proton chemical shifts of Ga^{3+}-complexes of nitrocatechol derivatives in water are presented relative to TMS. The proton positions are presented in Fig. 1 by numbering carbons to which the protons are bound. Δ is the difference of proton chemical shifts of Ga^{3+}-nitrocatechols from the nitrocatechols.

HEPES-saline (pH 7.4) at 25° (Table 1). To measure the reduction rate, dihydrolipoic acid was used as a reducing agent because the reduction by ascorbate or NADH at pH 7.4 was too slow to measure by oxygen electrode. The ratios of k_{Rd}/k_{Ox}, in order of magnitude, were citrate > catechol ≫ derivative **2** > **1**, **3**.

Iron binding by nitrocatechol derivatives and the physicochemical properties of the ion were studied by UV/vis absorption spectroscopy, ESR, and ^1H NMR. When the derivatives were mixed with ferric ion in aqueous solution, the color changed, depending on pH. At a pH of less than 1, the iron complexes were bluish light yellow, but as the pH increased, the color changed to brownish red. In UV/vis absorption spectroscopy of the aqueous solution, the absorbance maximum at ~700 nm changed to ~550 nm with increasing pH from 1.0 to 7.4. Typical absorption spectra at pH 4.5 and 7.4 are shown in Fig. 5. In DMSO, the ferric complexes showed an absorbance maximum at ~700 nm, which was virtually the same as that of aqueous acidic solutions, but the intensity was much stronger than that in aqueous acidic solution. All ferric complexes of nitrocatechol derivatives showed similar characteristics on UV/vis spectroscopy (Table 2). The absorbance maxima and molar extinction coefficients of ferric complexes of derivatives **1** and **3** were very similar, but in aqueous solution, the absorption band of iron-derivative **2** was in a lower energy region and the molar extinction coefficient was somewhat smaller than those of the others. Using the characteristic visible absorbance of ferric complexes, Job's plotting was done in HEPES-saline (pH 7.4) and DMSO (data not shown). In the ferric complex of derivative **2**, the molar ratio of iron to the derivative was 1:3 at pH 7.4; plotting for derivatives **1** and **3** was not done because the large absorption band of the derivative itself disturbed the measurement. In DMSO, the ratio was 1:1 for all nitrocatechol derivatives, IR spectra of iron complexes of nitrocatechol derivatives obtained as KBr disk also showed that the νOH (3250 and 3500 cm^{-1}) of the derivatives disappeared and the carbonyl groups remained (data not shown), which indicates that phenolic oxygens of the derivatives chelated iron and formed catechol-type iron complexes. Since the visible band of iron–catechol exhibits a blue shift depending on the pH changing the molar ratio of iron to catechol [14, 26], we inferred that in aqueous solution iron–nitrocatechol complexes changed the molar ratios of iron to nitrocatechol derivative from 1:1 to 1:3 with increasing pH:

$$Fe^{3+} + 3\ \text{nitrocat}^{2-} \rightarrow [Fe(\text{nitrocat})]^{+} + 2\ \text{nitrocat}^{2-} \rightarrow [Fe(\text{nitrocat})_2]^{-} + \text{nitrocat}^{2-} \rightarrow [Fe(\text{nitrocat})_3]^{3-}$$

and the visible absorption band is assigned to a nitrocatecholate → Fe^{3+} charge transfer transition [27].

ESR spectra of iron complexes of the nitrocatechol derivatives were recorded in HEPES-saline (pH 7.4) and DMSO (Fig. 6) at 200°K. In both solutions, the complexes mainly showed an ESR signal near g = 4.3 as expected for a transition between the middle Kramers' doublet of a rhombic high-spin iron(III) complex. The ESR signal near g = 4.3 had broad signals on both sides, which suggests that the complexes are not completely rhombic (E/D <1/3) [28]. This is also suggested by the fact that a weak ESR signal at lower field from the ground Kramers' doublet had a g value of less than 9.0. All iron complexes of nitrocatechol derivatives were in the ferric high-spin state with near-rhombicity.

For ^1H NMR study of the iron complexes, Ga^{3+} was used as a substitute for Fe^{3+} because Ga^{3+} has chemical properties similar to Fe^{3+} except for the diamagnetism [29, 30]. In DMSO, ^1H NMR of Ga^{3+} complexes of nitrocatechol derivatives (molar ratio = 1:1) was measured to confirm the binding sites. In the presence of Ga^{3+}, the proton signal (C3′ and C4′) of the phenolic hydroxyl group disappeared in derivatives **1** (Fig. 7) and **3**, which indicates that phenolic hydroxyl oxygens of the derivatives chelated Ga^{3+} and formed 1:1 gallium–nitrocatechol complexes. By integration of the ^1H NMR signal, it was found that ~70% of derivative **2** was the keto type and ~30% was the enol type. Proton shifts of Ga^{3+}-nitrocatechol complexes in DMSO are presented in Table 3. By Ga^{3+} binding, ring protons (C2′ and C6′) markedly shifted upfield, and protons of C6 also shifted in the same direction. Protons (C1 and C5 for **1** and **2**; C1 and C2 for **3**) at the end of the substituent shifted slightly. Similar results of proton chemical shifts were reported for enterobactin, a catechol-type siderophore [31]. In D_2O, ^1H NMR of Ga^{3+} complexes of nitrocatechol derivatives was measured at a 1:3 molar ratio of iron to the derivatives (Table 4). At pD 7.5, almost all ring protons (C2′ and C6′) of the derivatives shifted upfield the same as

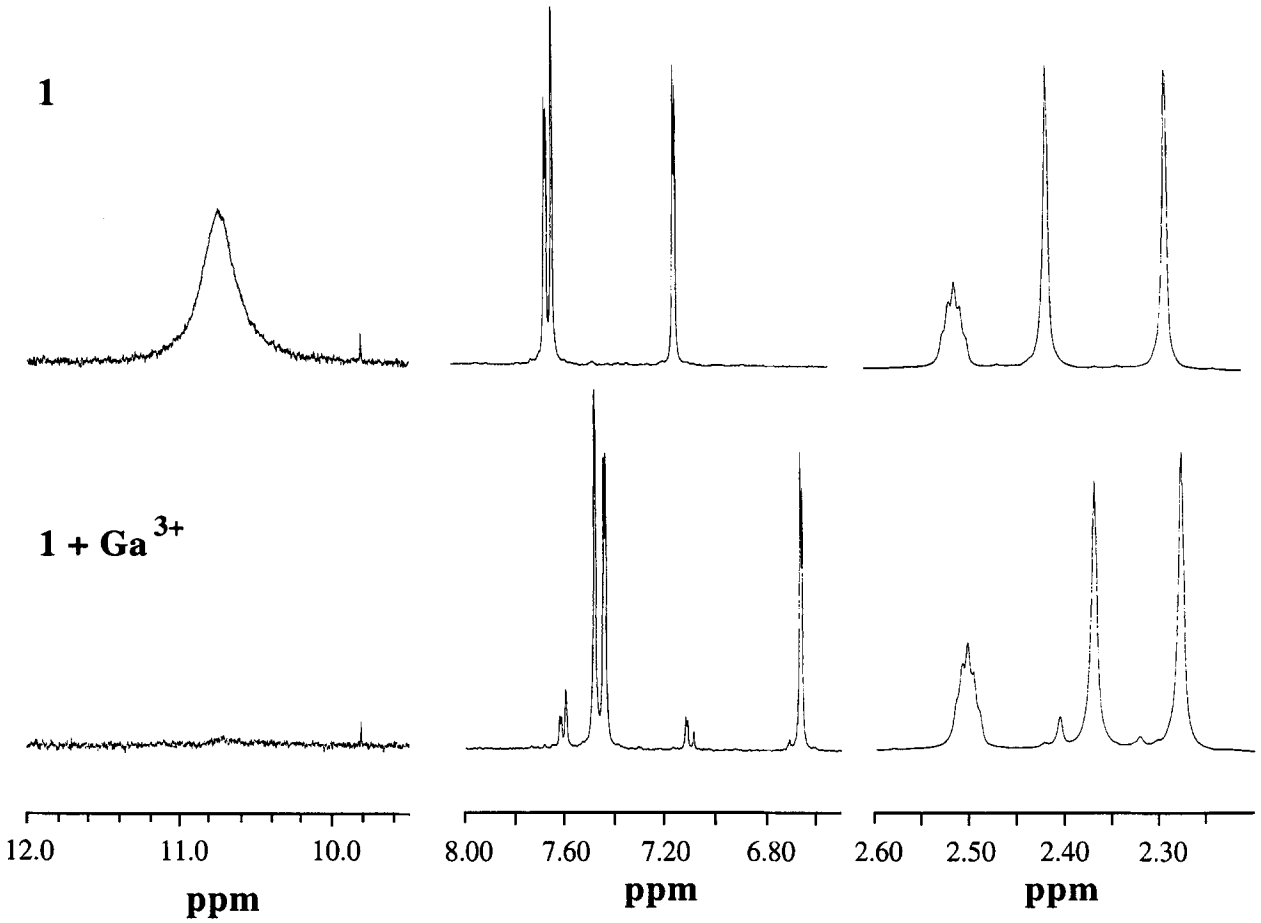

FIG. 7. ^{1}H NMR spectra of nitrocatechol derivative 1. The NMR spectra of nitrocatechol 1 (20 mM) were recorded at room temperature in DMSO-d_6 without and with Ga^{3+} (20 mM). Chemical shifts were measured using TMS as a reference, with downfield shift taken as positive.

in DMSO, suggesting that in aqueous solution at pD 7.5 all nitrocatechol derivatives form tris(nitrocatecholate) complexes. The methyl protons at the substituent end of nitrocatecholates shifted little because of the catechol-type complex.

We concluded that all nitrocatechol derivatives formed tris(nitrocatecholato)ferrate(III) in aqueous solution at pH 7.4 (Fig. 8); the iron was high-spin ferric.

DISCUSSION

We tested the effects of nitrocatechol derivatives on iron-induced free radical reactions. In iron-induced lipid peroxide-dependent lipid peroxidation, catechol and the derivatives showed inhibition in the same manner (Fig. 2), whereas in Fenton-like reactions iron complexes of nitrocatechol derivatives 1 and 3 did not generate hydroxyl radicals, but the iron complex of derivative 2 did (Figs. 3 and 4). Iron-catechol generated hydroxyl radicals more strongly than did citrate. Nitrocatechol derivatives 1 and 3 were the best chelators to protect against iron-induced free radical reactions. It is unlikely that the rates at which the generated ·OH reacts directly to the nitrocatechol derivatives are different between the derivatives because Marcocci *et al.* reported that derivatives 1 and 2 quenched oxygen free radicals in the same manner [18], and hydroxyl radical can react with almost all molecules with a diffusion-limited rate constant. Therefore, the different effects of catechol and nitrocatechol derivatives are attributed to the chelate structures and redox properties.

To elucidate the coordination structures of iron complexes of nitrocatechol derivatives, we studied the iron complexes in aqueous solution and DMSO. The structures of iron-nitrocatechol derivative complexes were different from iron–catechol complex. Catechol is reported to form tris(catecholato)ferrate(III) with iron at alkaline pH, but around pH 7.4 catechol predominantly forms a 1:2 complex with iron [14, 26, 32]. The nitrocatechol derivatives formed 1:3 complexes with iron at pH 7.4 (Fig. 8). The nitrocatechol derivatives have lower pK_a values of the phenolic hydroxyl groups than catechol because of an electrophilic nitro group in dihydroxylbenzene moiety [18] and can make 1:3 complexes with iron at pH 7.4, which is more beneficial to sequester iron and prohibit the iron from the approach of

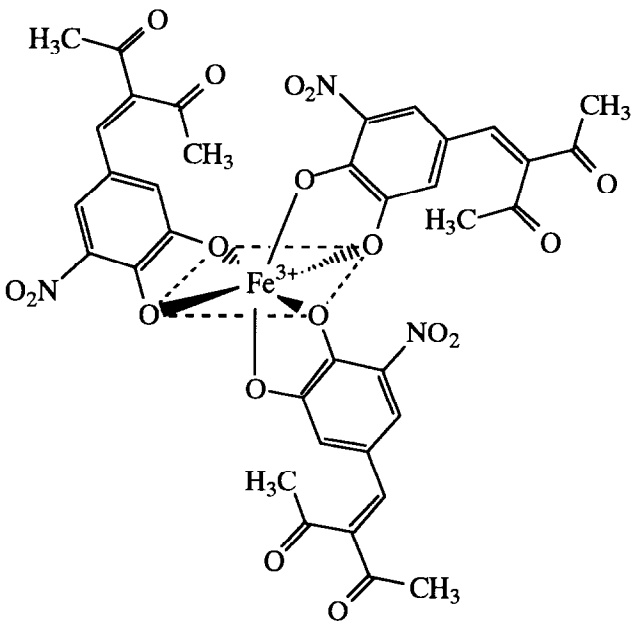

FIG. 8. Proposed structure of the iron complex of nitrocatechol derivative 1 at pH 7.4.

the reactants in biological systems. In a molecule of 1:2 iron–catechol complex is a space through which a small reactant such as hydrogen peroxide can approach the chelated iron, but lipid peroxides, which are larger, do not approach the catalytic iron by the steric effect [33].

The redox properties of the iron complexes are important in the free radical generation by transition metals. Considering the equilibrium of ferric and ferrous complexes:

$$Fe^{3+} + e^- \underset{k_{-1}}{\overset{k_1}{\rightleftharpoons}} Fe^{2+}$$

the ratio of k_1/k_{-1} is related to the reduction potential, $\Delta E = -\Delta G/F = RT \ln(k_1/k_{-1})/F$, were F is the Faraday constant. Using the ratio k_{Rd}/k_{Ox} as a substitute for k_1/k_{-1}, the k_{Rd}/k_{Ox} may also be related to the reduction potential. We evaluated the redox properties of the iron complexes by the k_{Rd}/k_{Ox} ratios (Table 1). Iron complexes of all nitrocatechol derivatives had much lower ratios than iron citrate, which is consistent with low reduction potentials of catechol-type iron complexes [11–13]. Iron-catechol showed a higher reduction potential than iron–nitrocatechols because of the different coordination structure. Iron complexes of nitrocatechol derivatives 1 and 3 showed the same k_{Rd}/k_{Ox} ratio, while iron complex of nitrocatechol derivative 2 had a higher ratio, which suggested that iron–nitrocatechol 2 has a higher reduction potential than the other iron–nitrocatechols (1 and 3). It is reported that iron phenolate with conjugated substituent has a lower reduction potential than the corresponding iron phenolate without the conjugation [34]. Nitrocatechol derivatives 1 and 3 have conjugation substitutes, but derivatives 2 does not. This fact is reasonably explained by molecular orbital considerations, that is, a catechol with a conjugation substituent has higher energy of HOMO than the corresponding one without the conjugation, and iron d oribtals in catechol-type iron complexes are sensitive to the HOMO [35, 36]. As shown in the λ_{max} data (Table 2), the energy gap of ligand-to-metal charge transfer ($\pi \rightarrow d_\pi$) of iron–nitrocatechol 2 was larger than those of iron–nitrocatechols 1 and 3. Therefore, we inferred that iron–nitrocatechol 2 has a higher reduction potential than iron–nitrocatechols 1 and 3, and generated hydroxyl radical in a Fenton-like reaction. The reaction rates of ligand exchange of iron–nitrocatechols may not be so important because iron chelated by the derivatives was high-spin ferric in iron–nitrocatechols (Fig. 6), and all the high-spin iron complexes may be ligand-exchange-labile [37].

In this study we showed that nitrocatechol derivatives with a conjugation structure are promising candidates for therapy of so-called "free radical diseases." In addition to the radical scavenging effects, they have strong thermodynamic stabilities for iron, and the chelated iron has no catalytic activity for free radical generation because the iron complexes prefer the ferric state to the ferrous one due to the low reduction potentials.

This work was supported by National Institutes of Health (CA 47597) and Orion-Farmos Pharmaceuticals (Espoo, Finland). We thank Dr. M. Mizuno for help with chemical interpretation and Dr. N. Fujitake for IR spectroscopy.

References

1. Halliwell B and Gutteridge JMC, *Free Radicals in Biology and Medicine*. Clarendon, Oxford, 1989.
2. Millar DM, Buettner GR and Aust SD, Transition metals as catalysts of "autoxidation" reactions. *Free Radic Biol Med* **8:** 95–108, 1990.
3. Stadtman ER, Metal ion-catalyzed oxidation of proteins: Biochemical mechanism and biological consequences. *Free Radic Biol Med* **9:** 315–325, 1990.
4. Lauffer RB, *Iron and Human Disease*. CRC Press, Boca Raton, 1992.
5. Halliwell B and Gutteridge JMC, Role of free radicals and catalytic metal ions in human disease: An overview. *Methods Enzymol* **186:** 1–85, 1990.
6. Yamazaki I and Piette LH, ESR spin-trapping studies on the reaction of Fe^{2+} ions with H_2O_2-reactive species in oxygen toxicity in biology. *J Biol Chem* **265:** 13589–13594, 1990.
7. Yamazaki I and Piette LH, EPR spin-trapping study on the oxidizing species formed in the reaction of the ferrous ion with hydrogen peroxide. *J Am Chem Soc* **113:** 7588–7593, 1991.
8. Rush JD, Cyr JE, Zhao ZW and Bielski BHJ, The oxidation of phenol by ferrate(VI) and ferrate(V). A pulse radiolysis and stopped-flow study. *Free Radic Res* **22:** 349–360, 1995.
9. Jacob A and Worwood M, *Iron in Biochemistry and Medicine*. Academic Press, London, 1980.
10. Williams RJP, *An Introduction to the Nature of Iron Transport and Storage*. CRC Press, Boca Raton, 1990.
11. Buettner GR, The pecking order of free radicals and antioxidants: Lipid peroxidation, α-tocopherol, and ascorbate. *Arch Biochem Biophys* **300:** 535–543, 1993.
12. O'Brien IG, Cox GB and Gibson F, Enterochelin hydrolysis

and iron metabolism in *Escherichia coli*. *Biochim Biophys Acta* **237:** 537–549, 1971.
13. Cooper SR, McArdle JV and Raymond KN, Siderophore electrochemistry: Relation to intracellular iron release mechanism. *Proc Natl Acad Sci USA* **75:** 3551–3554, 1978.
14. Avdeef A, Sofen SR, Bregante TL and Raymond KN, Coordination chemistry of microbial iron transport compounds. 9. Stability constants for catechol models of enterobactin. *J Am Chem Soc* **100:** 5362–5370, 1978.
15. Raymond KN, Isied SS, Brown LD, Fronczek FR and Nibert JH, Coordination isomers of biological iron transport compounds. VI. Models of the enterobactin coordination site. A crystal field effect in the structure of potassium tris(catecholato)chromate(III) and -ferrate(III) sesquihydrates, $K_3[M(O_2C_6H_4)_3] \cdot 1.5H_2O$, M = Cr, Fe. *J Am Chem Soc* **98:** 1767–1774, 1976.
16. Matzanke BF, Mueller-Matzanke G and Raymond KN, *Siderophore-Mediated Iron Transport*. VHC Publishers, New York, 1989.
17. Suzuki YJ, Tsuchiya M, Asaad S, Kagan VE and Packer L, Antioxidant properties of nitecapone (OR-462). *Free Radic Biol Med* **13:** 517–525, 1992.
18. Marcocci L, Suzuki YJ, Tsuchiya M and Packer L, Antioxidant activity of nitecapone and its analog OR-1246: Effect of a structural modification on antioxidant action. *Methods Enzymol* **234:** 538–553, 1994.
19. Haramaki N, Stewart DB, Aggarwal S, Kawabata T and Packer L, Role of ascorbate in protection by nitecapone against cardiac ischemia–reperfusion injury. *Biochem Pharmacol* **50:** 839–843, 1995.
20. Green MJ and Hill AO, Chemistry of dioxygen. *Methods Enzymol* **105:** 3–22, 1984.
21. Hogeboom GH, Fractionation of cell components of animal tissues. *Methods Enzymol* **1:** 16–19, 1955.
22. Lowry OH, Rosebrough NJ, Farr AL and Randall RJ, Protein measurement with the Folin phenol reagent. *J Biol Chem* **193:** 265–275, 1951.
23. Ohkawa H, Ohishi N and Yagi K, Assay for lipid peroxides in animal tissues by thiobarbituric acid reaction. *Anal Biochem* **95:** 351–358, 1979.
24. Kawabata T, Tritschler H-J and Packer L, Reaction of (*R,S*)-dihydrolipoic acid and homologs with iron. *Methods Enzymol* **251:** 325–332, 1995.
25. Wertz JE and Bolton JR, *Electron Spin Resonance. Elementary Theory and Practical Applications*. Chapman & Hall, New York, 1986.
26. Aplincourt M, Gerard C, Hugel RP, Pierrard JC, Rimbault J, Bertrandie A, Magny B and Siret PJ, Metal cation–ligand interactions of catechols of biological importance. I. Stability of iron(III) dihydroxybenzamide complexes which are related to cephalosporins bearing at C3′ a catechol group. *Polyhedron* **11:** 1161–1168, 1992.
27. Salama S, Stong JD, Neiland JB and Sprio TG, Electronic and resonance raman spectra of iron(III) complexes of enterobactin, catechol, and *N*-methyl-2,3-dihydroxybenzamide. *Biochemistry* **17:** 3781–3785, 1978.
28. Aasa R, Powder line shapes in the electron paramagnetic resonance spectra of high-spin ferric complexes. *J Chem Phys* **52:** 3919–3930, 1970.
29. Borgias BA, Barclay SJ and Raymond KN, Structural chemistry of gallium(III). Crystal structures of $K_3[Ga(catecholate)_3] \cdot 1.5H_2O$ and $[Ga[benzohydroxamate)_3] \cdot H_2O \cdot CH_3CH_2OH$. *J Coord Chem* **15:** 109–123, 1986.
30. Cotton FA and Wilkinson G, *Advanced Inorganic Chemistry*. John Wiley, New York, 1988.
31. Llinas M, Wilson DM and Neilands JB, Effect of metal binding on the conformation of enterobactin. A proton and carbon-13 nuclear magnetic resonance study. *Biochemistry* **12:** 3836–3843, 1973.
32. Mentasti E and Pelizzetti E, Reaction between iron(III) and catechol (*o*-dihydroxybenzene). Part 1. Equilibria and kinetics of complex formation in aqueous acid solution. *J Chem Soc Dalton Trans* 2605–2614, 1973.
33. Traylor TG and Ciccone JP, Mechanism of reaction of hydrogen peroxide and hydroperoxides with iron(III) porphyrins. Effects of hydroperoxide structure on kinetics. *J Am Chem Soc* **111:** 8413–8420, 1989.
34. Ramesh K and Mukherjee R, Trends in the spectral and redox potential data of mononuclear iron(III) (S = 5/2) phenolate complexes. *J Chem Soc Dalton Trans* 83–89, 1992.
35. Gordon DJ and Fenske RF, Theoretical study of *o*-quinone complexes of iron. *Inorg Chem* **21:** 2916–2923, 1982.
36. Pyrz JW, Roe AL, Stern LJ and Que LJ, Model studies of iron-tryosinate protein. *J Am Chem Soc* **107:** 614–620, 1985.
37. Basolo F and Pearson RG, *Mechanisms of Inorganic Reactions: A Study of Metal Complexes in Solution*. John Wiley, New York, 1967.